ChemComm

Hydrogen-Bonded Nickel(I) Complexes

Journal:	*ChemComm*
Manuscript ID	CC-COM-10-2020-007216.R1
Article Type:	Communication

COMMUNICATION

Hydrogen-Bonded Nickel(I) Complexes

Jessica R. Wilson, [a] Matthias Zeller [b] and Nathaniel K. Szymczak [a]*

Received 00th January 20xx,
Accepted 00th January 20xx

DOI: 10.1039/x0xx00000x

A series of nickel(II) tris(2-pyridylmethyl)amine (TPA) complexes featuring appended hydrogen bonds (H-bonds) to halides (F, Cl, Br) was synthesized and charcterized. Reduction to the corresponding nickel(I) state provided access to an unusual nickel(I) fluoride complex stabilized by H-bonds, enabling structural and spectroscopic characterization.

Exploration into redox interconversions of nickel-based coordination complexes is motivated by relevance to both the bioinorganic[1] and organometallic fields.[2] In the latter, Ni has recently emerged as a prominent metal with catalytic applications. A key difference between Ni and its congeners (Pd and Pt) is the propensity to undergo single- rather than double-electron transfer during bond cleavage reactions, a feature that has facilitated an expansion of the available chemical landscape.[3] Single electron reduction of the common Ni(II) state affords Ni(I) complexes, many of which react with a variety of small molecule substrates.[4] One feature typically used to enable the isolation of higher-coordinate Ni(I) complexes is incorporation of supporting ligands that contain soft donor and/or π-acceptor groups (e.g. phosphine, CO, CN^-).[5]

In contrast to synthetic systems, less ligand diversity is available within the active sites of metalloenzymes, and stabilization of reduced states/substrates/intermediates is augmented by a network of secondary sphere interactions.[6] These secondary sphere interactions are critical to the function of many biological transformations including H^+/e^- interconversions,[7] and CO_2 reduction.[8] To emulate this design principle, study, and ultimately develop synthetic analogues, complexes containing appended H-bond donors are increasingly used in biomimetic design[6a,9] and catalytic transformations.[9b,10] However, a key limitation in synthetic systems is the general incompatibility of H-bond donors with low-valent metal complexes.[11] Thus, most studies are limited to mid- to high-oxidation-state transformations, and/or undergo proton transfer if reduced to a low-valent state.[12] One synthetic strategy to achieve reductive stability is to use weakly acidic H-bond donors that can engage with metal-coordinated substrates.[13] Such donor/acceptor interactions are straightforward to access and study using halides, the strongest acceptor of which is fluoride.

Low valent late transition metal-fluoride complexes are uncommon,[14] a consequence of electron pair repulsion between occupied *p*- and *d*- orbitals on fluorine and the metal, respectively.[15] This destabilizing interaction can be overcome by engaging secondary sphere H-bonds with fluoride, which alleviates the filled-filled repulsive interactions through donor/acceptor interactions. We recently demonstrated this and related principles using –EH-appended TPA based ligands (E = O, NAr),[16] and in one case, the secondary coordination sphere served to capture fluoride in a molecule that would otherwise undergo dissociation.[16b] Although both –NHAr and –OH groups engage in highly directed H-bonding interactions,[16,17a] –NHAr groups are less acidic, and thus, more stable at reduced potentials.[17b] We hypothesized that reductively stable, directed H-bonds could provide necessary stabilization to isolate low valent metal complexes, including Ni(I) (Fig. 1).

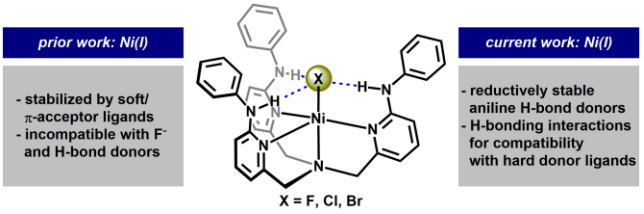

Fig. 1 Outline of design strategy to stabilize low-valent Ni complexes with H-bonds.

We targeted a series of nickel(II) halide complexes containing the tris(6-phenylamino-2-pyridylmethyl)amine ligand (L^H). NiX_2 compounds, where X = Cl or Br, were prepared

[a] Department of Chemistry, University of Michigan, Ann Arbor, Michigan 48109, United States
[b] H.C. Brown Laboratory, Department of Chemistry, Purdue University, West Lafayette, Indiana 47907, United States

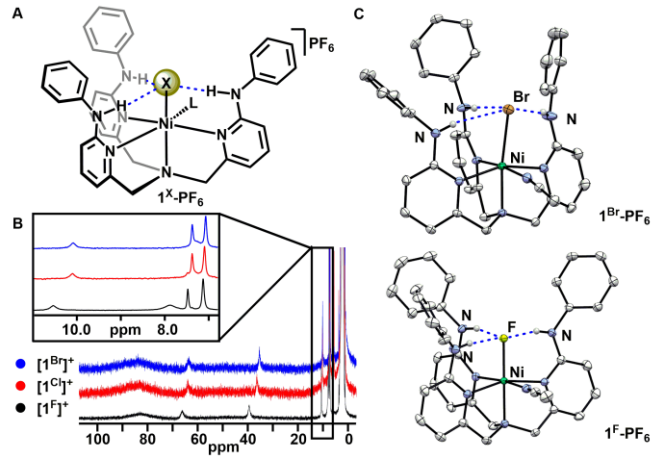

Fig. 2 (A) General structure of complexes $\mathbf{1^X\text{-}PF_6}$, L = CH_3CN. (B) Paramagnetic ^1H NMR spectra of series $\mathbf{1^X\text{-}PF_6}$. (C) Molecular structures (50% probability) of $\mathbf{1^{Br}\text{-}PF_6}$, and $\mathbf{1^F\text{-}PF_6}$ (counterions excluded for clarity).

by metalation of L^H with either $NiCl_2{\bullet}6H_2O$ or $NiBr_2$(DME) in CH_3CN solvent. After 1 h, the precipitated compounds were decanted to afford $NiCl_2L^H$ and $NiBr_2L^H$ in moderate to high yields. To prepare the fluoride congener, NiF_2L^H, 2 equiv. CsF were combined with $NiCl_2L^H$, and a pale blue-green solid was isolated after 24 h (see ESI). The ^1H NMR spectrum revealed broad resonances ranging from 7 to 85 ppm.[18] Structural characterization of $NiCl_2L^H$ revealed a monomeric octahedral complex (see ESI). Salt metathesis of NiX_2L^H with $TlPF_6$ or $TlBAr'_4$ (BAr'_4 = tetrakis[3,5-bis(trifluoromethyl)phenyl]borate) afforded the monohalide species $[NiXL^H]^+$, $\mathbf{[1^X]^+}$.

Complexes $\mathbf{[1^X]^+}$ were characterized by ^1H NMR and electronic absorption spectroscopy. The soluble, paramagnetic complexes exhibit C_3-symmetric ^1H NMR spectra, similar to previously characterized Ni(II)TPA complexes (Fig. 2).[19] Although $\mathbf{1^{Br}\text{-}BAr'_4}$ and $\mathbf{1^{Cl}\text{-}BAr'_4}$ are similar (Br: 656 nm, ε = 13 $cm^{-1}M^{-1}$, ~1075 nm, ε = 20 $cm^{-1}M^{-1}$; Cl: 638 nm, ε = 19 $cm^{-1}M^{-1}$, 1046 nm, ε = 28 $cm^{-1}M^{-1}$), complex $\mathbf{1^F\text{-}BAr'_4}$ features bands that are shifted to higher energy (581 nm, ε = 11 $cm^{-1}M^{-1}$; 937 nm, ε = 15 $cm^{-1}M^{-1}$), consistent with higher ligand field strength.[20,21]

Across the halide series, we evaluated the structural metrics obtained from single crystals of $\mathbf{1^{Br}\text{-}PF_6}$, $\mathbf{1^{Cl}\text{-}PF_6}$, and $\mathbf{1^F\text{-}PF_6}$. All three complexes exhibit octahedral geometry, with a coordinated CH_3CN molecule. In all cases, the halide engages in trifurcated H-bonding interactions to the appended aniline –NH groups, with average N-X distances decreasing from -Br to -F (Br = 3.271 Å, Cl = 3.159 Å, F = 2.731 Å). These results are consistent with moderate H-bond strength and increasing H-bond accepting ability across the halide series, Br < Cl < F.[22] Of note, complexes $\mathbf{1^{Br}\text{-}PF_6}$ and $\mathbf{1^{Cl}\text{-}PF_6}$ crystallize in the same space group ($P2_1/c$) and are isomorphous, in contrast to $\mathbf{1^F\text{-}PF_6}$ ($Pbca$) (Fig. 2; for overlaid structures, see ESI). The similarities between $\mathbf{1^{Br}\text{-}PF_6}$ and $\mathbf{1^{Cl}\text{-}PF_6}$ may be a composite of H-bonding as well as crystal packing forces, which we note can have similar strengths.[23]

We interrogated H-bonding interactions in $\mathbf{1^X}$ by examining the NH stretching frequencies in the infrared spectra.[24] For the strongest acceptor, fluoride, we observed a shift in the ν_{NH} from 3400 cm^{-1} to 3250 cm^{-1} for L^H and $\mathbf{1^F\text{-}BAr'_4}$, respectively, consistent with an H-bond interaction between –NH and the F-Ni (for ν_{NH} assignment, see ESI).[16a] Across the halide series, ν_{NH} decreases as F > Cl > Br, which is opposite from their respective acceptor abilities. We attribute this feature to distortions from planarity of the aniline N atoms as the halide size increases (see ESI).[25]

Although $\mathbf{[1^X]^+}$ exhibit octahedral solid-state structures, room temperature ^1H NMR spectroscopy experiments indicated C_3-symmetry. The spectra of $\mathbf{1^{Cl}\text{-}PF_6}$ and $\mathbf{1^{Br}\text{-}PF_6}$ are nearly identical, in contrast to $\mathbf{1^F\text{-}PF_6}$, which exhibits resonances that are shifted downfield (see Fig. 2). To assess the role(s) of fluxional exchange processes on the solution structure, we performed a variable temperature ^1H NMR experiment. When a THF solution of $\mathbf{1^F\text{-}PF_6}$ was cooled to -75°C, additional resonances appeared (30-70 ppm). These additional resonances were replicated at room temperature by adding 1 equiv. of a strongly coordinating ligand, *N,N*-dimethylaminopyridine (see ESI). Collectively, these results are consistent with a dynamic ligand association in solution, in which the 5-coordinate Ni(II) species coordinates a sixth ligand, which imparts a geometrical change from C_3-symmetry to octahedral geometry: the latter geometry is common in related Ni(II)TPA complexes.[26]

In contrast to the ~100 structurally reported Ni(II)TPA (or TPA-related) complexes, there are no structurally characterized low valent variants.[27] To our knowledge, the only report of a Ni(I)TPA complex forms from $[(Ni(Me_2\text{-}TPA)(H)_2]^{2+}$, which was not characterized in the solid state.[19b] We employed cyclic voltammetry experiments to assess the accessibility of a reduced Ni(I) state. The free ligand, L^H, is reductively stable up to -3 V (glassy carbon vs. Fc^+/Fc; 0.1M $[NBu_4][OTf]$ in CH_3CN). Complexes $\mathbf{1^X\text{-}BAr'_4}$ exhibit a reversible reduction event at $E_{1/2}$ = -1.81 V, -1.56 V and -1.48 V for $\mathbf{1^F\text{-}BAr'_4}$, $\mathbf{1^{Cl}\text{-}BAr'_4}$ and $\mathbf{1^{Br}\text{-}BAr'_4}$, respectively (Fig. 3).

Chemical reduction of $\mathbf{1^F\text{-}PF_6}$ with potassium graphite (KC_8) in THF at -78 °C immediately formed a dark blue-green complex ($\mathbf{2^F}$). Reductions of $\mathbf{1^{Cl}\text{-}PF_6}$ and $\mathbf{1^{Br}\text{-}PF_6}$ proceeded similarly to afford $\mathbf{2^{Cl}}$ (blue) and $\mathbf{2^{Br}}$ (purple). These complexes gradually decompose in THF at room temperature ($t_{1/2}$ = 5.1 h; $\mathbf{2^{Cl}}$) but are stable at lower temperatures (<-35 °C). Characterization of the series of $\mathbf{2^x}$ by electronic absorption spectroscopy revealed a single broad absorbance in the visible region (for $\mathbf{2^{Cl}}$, λ = 593 nm, ε = 1950 $cm^{-1}M^{-1}$; for $\mathbf{2^F}$, λ = 706 nm, ε = 1444 $cm^{-1}M^{-1}$; and $\mathbf{2^{Br}}$, λ = 550 nm, ε = 3030 $cm^{-1}M^{-1}$). An X-band EPR spectrum of $\mathbf{2^{Cl}}$ (110 K) revealed *g* values of 2.28, 2.21, and 2.02, consistent with a d^9 Ni(I) system,[19b,28] with similar spectra for $\mathbf{2^F}$ and $\mathbf{2^{Br}}$ (see ESI).[29]

The solid-state structure of $\mathbf{2^F}$ revealed a trigonal bipyramidal geometry (τ_5 = 0.94)[29] with an axial fluoride ligand. In this arrangement, the three appended –NH groups of the pendent anilines engage in moderately strong H-bonding interactions with the Ni-F (avg. N-X bond distance = 2.666 Å).[30] Upon reduction of $\mathbf{1^F\text{-}PF_6}$ to $\mathbf{2^F}$, the Ni-F distance increases from 2.007(1) Å to 2.097(2) Å. We propose that elongation of the Ni-F bond imparts a higher H-bond acceptor strength, which is consistent with the shorter –NH-F contacts in $\mathbf{2^F}$, compared to $\mathbf{1^F\text{-}PF_6}$.[31] Although most reported Ni(I) complexes contain soft donor ligands, the primary coordination sphere comprising $\mathbf{2^F}$ contains comparatively hard donors. Complex $\mathbf{2^F}$ represents a

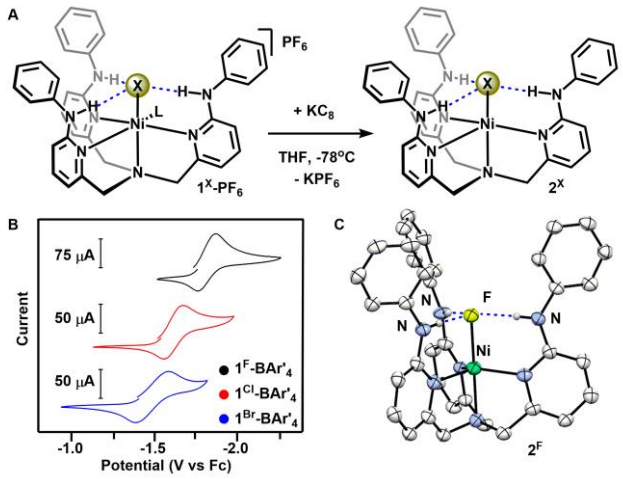

Fig. 3. (A) Synthesis of $\mathbf{2^X}$ (X = F, Cl, Br). (B) Cyclic voltammetry of series $\mathbf{1^X\text{-}BAr'_4}$, showing reversible Ni(II/I) couple. (C) Molecular structure (50% probability) of $\mathbf{2^F}$ (co-crystallized solvent molecules excluded for clarity).

structurally rare example of a 5-coordinate Ni(I) complex featuring halide ligands,[28b,32] a feature that we propose is enabled by directed H-bonding interactions. Furthermore, $\mathbf{2^F}$ represents the first example of a Ni(I) complex containing secondary sphere H-bonding groups.

Several examples of formally Ni(I) complexes containing pyridine-based ligands are best described as Ni(II)-L•, rather than Ni(I).[33] Wieghardt and co-workers showed that these two limiting cases can be distinguished by scrutinizing the pyridine intraligand bond distances.[34] The bond lengths of the pyridines in $\mathbf{2^F}$ and $\mathbf{1^F\text{-}PF_6}$ are normal for both C–C ($\mathbf{2^F}$: 1.387(5), $\mathbf{1^F\text{-}PF_6}$: 1.390(3)) and C–N bonds ($\mathbf{2^F}$: 1.353(5), $\mathbf{1^F\text{-}PF_6}$: 1.56(2)), (typical values for C–C and C–N: 1.38 ± 0.1 Å and 1.35 ± 0.1 Å, respectively), which is inconsistent with pyridine-based reduction.[34a] These crystallographic bond metrics, along with the EPR spectrum are consistent with a Ni-centered metalloradical (*vide supra*) for complex $\mathbf{2^F}$ (and by extension, $\mathbf{2^{Cl}}$ and $\mathbf{2^{Br}}$).

To assess the requirement of H-bonding interactions with Ni-X to isolate Ni(I) complexes, we evaluated the analogous syntheses using unsubstituted TPA. $[NiCl(TPA)]^+$ was prepared in quantitative yield from $NiCl_2TPA$,[19a] when subjected to analogous reaction conditions as for $\mathbf{[1^{Cl}]^+}$. In contrast, when conditions used to prepare NiF_2L^H were applied to TPA, we did not observe the formation of NiF_2TPA, in line with the absence of prior reports. Reduction of $[NiCl(TPA)]BAr'_4$ with KC_8 afforded a deep teal solution, which was characterized by ^1H NMR, electronic, and EPR spectroscopies. The electronic absorption spectrum features a single broad absorbance at 720 nm (ε = 4271 $cm^{-1}M^{-1}$).[35] The X-band EPR spectrum (110 K) reveals *g* values of 2.10, 2.20, and 2.09. These data are similar to a prior report that analyzed an *in situ* generated $Ni(I)(CH_3CN)_2(Me_2\text{-}TPA)$ at low temperature (7 K).[19b] Despite their spectroscopic similarities, the solution behaviors of $\mathbf{2^{Cl}}$ and NiCl(TPA) are distinct. The unsubstituted variant is prone to rapid decomposition ($t_{½}$ = 0.3 h at 25°C) in comparison to $\mathbf{2^{Cl}}$ ($t_{1/2}$ = 5.1 h). These data indicate large differences in stability ($\mathbf{2^{Cl}}$ is >15 x more stable than NiCl(TPA)), a feature that we propose is due to halide H-bonding interactions present in $\mathbf{2^{Cl}}$.

Given the high affinity of halides to engage in H-bonding interactions to the pendent aniline groups, we sought to investigate dehalogenation reactivity induced by the strongest H-bond acceptor halide, fluoride. We accessed defluorination reactions using a putative halide-free $\mathbf{[2]^+}$ by adding $TlBAr'_4$ to a solution of $\mathbf{2^{Br}}$ to -78°C, followed by $NaBF_4$. We observed $\mathbf{[1^F]^+}$ as the *only* NMR active species.

Directed H-bonding interactions to fluoride have been shown to induce E-F bond cleavage from B-F[36] and C-F[37] moieties. The favorability of such reactions may be predicted using fluoride ion affinity values (FIAs). Since fluoride abstraction from BF_4^- (FIA of BF_3 = 82.7 kcal mol^{-1})[38] occurs readily in this system, the FIA value provides insight into the fluorophilicity of the H-bonding pocket of $\mathbf{[1^F]^+}$. In contrast to $NaBF_4$, $NaSbF_6$ did not form $\mathbf{[1^F]^+}$, consistent with a higher fluorophilicity of SbF_5 (118.5 kcal mol^{-1})[38] than fluoride-free $\mathbf{[1]^+}$. Finally, we evaluated defluorination reactions with organic substrates containing N-F bonds. Using the protocol described above with both neutral N-fluorosulfonimide (BDE = 63.4 kcal mol^{-1})[39] and ionic 1-fluoro-2,4,6-trimethylpyridnium triflate (BDE = 77.8 kcal mol^{-1})[39] (see Fig. 4), we observed exclusive formation of $\mathbf{[1^F]^+}$ (see ESI).[40] In contrast, reactions using NiCl(TPA) afforded multiple species. The disparate reactivity of otherwise identical complexes containing distinct secondary coordination sphere environments highlights the reactivity-controlling role of H-bonding interactions and fluoride ion affinity to bias a defluorination reaction.

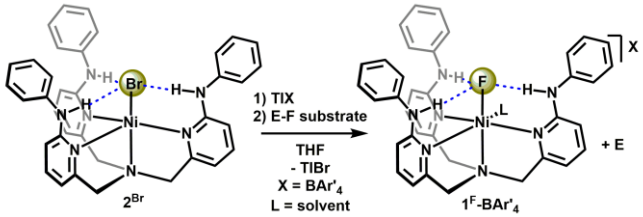

Fig. 4. Reaction of $\mathbf{2^{Br}}$ with E-F substrates to form $\mathbf{1^F\text{-}BAr'_4}$ (E = B, N)

In summary, we prepared a series of Ni(II) complexes featuring H-bonds to halides. These secondary sphere interactions are critical for the isolation and enhanced stability of Ni(I) complexes. The H-bond interactions remain intact, even at < -1.8 V (vs Fc), showcasing the reductive stability of appended aniline H-bond donors. The H-bond donor/acceptor interactions represent an attractive strategy wherein classically hard ligands, such as fluoride, can be rendered compatible with highly reduced and soft late metals.

This work was supported by the NIH (1R35GM136360-01), a Rackham Graduate Student Research Grant (J. R. W.), and the NSF (CHE-0840456, and CHE-1625543) for X-ray instrumentation. N. K. S. is a Camille Dreyfus Teacher-Scholar. We thank Dr. Jeff Kampf for X-ray assistance.

Conflicts of interest

There are no conflicts to declare.

Notes and references

1 J. L. Boer, S. B. Mulrooney and R. P. Hausinger, *Arch. Biochem. Biophys.*, 2014, **544**, 142-152.
2 S. Z. Tasker, E. A. Standley and T. F. Jamison, *Nature*, 2014, **509**, 299-309.
3 F. S. Han, *Chem Soc Rev*, 2013, **42**, 5270-5298.
4 (*a*) P. Zimmermann and C. Limberg, *J. Am. Chem. Soc.*, 2017, **139**, 4233-4242; (*b*) K. Nag and A. Chakravorty, *Coord. Chem. Rev.*, 1980, **33**, 87-147; (*c*) M. T. Kieber-Emmons and C. G. Riordan, *Acc. Chem. Rev.*, 2007, **40**, 618-625.
5 C. Y. Lin and P. P. Power, *Chem Soc Rev*, 2017, **46**, 5347-5399.
6 A. S. Borovik, *Acc. Chem. Res.*, 2005, **38**, 54-61
7 (*a*) S. Shima, O. Pilak, S. Vogt, M. Schick, M. S. Stagni, W. Meyer-Klaucke, E. Warkentin, R. K. Thauer and U. Ermler, *Science*, 2008, **321**, 572-575; (*b*) W. Lubitz, H. Ogata, O. Rüdiger and E. Reijerse, *Chem. Rev.*, 2014, **114**, 4081-4148; (*c*) T. Hiromoto, E. Warkentin, J. Moll, U. Ermler and S. Shima, *Angew. Chem. Int. Ed.*, 2009, **48**, 6457-6460; (*d*) G. F. Huang, T. Wagner, M. D. Wodrich, K. Ataka, E. Bill, U. Ermler, X. L. Hu and S. Shima, *Nat. Catal.*, 2019, **2**, 537-543. (*e*) C. M. Moore, E. W. Dahl and N. K. Szymczak, *Curr. Opin. Chem. Biol.*, 2015, **25**, 9-17.
8 J.-H. Jeoung and H. Dobbek, *Science*, 2007, **318**, 1461-1464.
9 (*a*) Z. Han, K. T. Horak, H. B. Lee and T. Agapie, *J. Am. Chem. Soc.*, 2017, **139**, 9108-9111; (*b*) C. L. Ford, Y. J. Park, E. M. Matson, Z. Gordon and A. R. Fout, *Science*, 2016, **354**, 741; (*c*) V. Yadav, J. B. Gordon, M. A. Siegler and D. P. Goldberg, *J. Am. Chem. Soc.*, 2019, **141**, 10148-10153.
10 (*a*) C. M. Moore and N. K. Szymczak, *Chem. Commun.*, 2013, **49**, 400-402; (*b*) E. W. Dahl, T. Louis-Goff and N. K. Szymczak, *Chem. Commun.*, 2017, **53**, 2287-2289; (*c*) Eva M. Nichols, J. S. Derrick, S. K. Nistanaki, P. T. Smith and C. J. Chang, *Chem. Sci.*, 2018, **9**, 2952-2960; (*d*) M. Delgado and J. D. Gilbertson, *Chem. Commun.*, 2017, **53**, 11249-11252; (*e*) C. Costentin, S. Drouet, M. Robert and J.-M. Savéant, *Science*, 2012, **338**, 90; (*f*) I. Azcarate, C. Costentin, M. Robert and J.-M. Savéant, *J. Am. Chem. Soc.*, 2016, **138**, 16639-16644; (*g*) M. L. Pegis, B. A. McKeown, N. Kumar, K. Lang, D. J. Wasylenko, X. P. Zhang, S. Raugei and J. M. Mayer, *ACS Cent. Sci.*, 2016, **2**, 850-856 (*h*) G. P. Connor, N. Lease, A. Casuras, A. S. Goldman, P. L. Holland and J. M. Mayer, *Dalton Trans.*, 2017, **46**, 14325-14330.
11 (*a*) R. H. Morris, *Chem. Rev.*, 2016, **116**, 8588-8654; (*b*) S. E. Creutz and J. C. Peters, *Chem. Sci.*, 2017, **8**, 2321-2328; (*c*) C. J. Weiss, J. D. Egbert, S. Chen, M. L. Helm, R. M. Bullock and M. T. Mock, *Organometallics*, 2014, **33**, 2189-2200; (*d*) J. P. Shanahan and N. K. Szymczak, *J. Am. Chem. Soc.*, 2019, **141**, 8550-8556.
12 (*a*) S. E. Creutz and J. C. Peters, *J. Am. Chem. Soc.*, 2014, **136**, 1105-1115; (*b*) P. Bhattacharya, Z. M. Heiden, E. S. Wiedner, S. Raugei, N. A. Piro, W. S. Kassel, R. M. Bullock and M. T. Mock, *J. Am. Chem. Soc.*, 2017, **139**, 2916-2919.
13 J. P. Shanahan, D. M. Mullis, M. Zeller and N. K. Szymczak, *J. Am. Chem. Soc.*, 2020, **142**, 8809-8817.
14 J. H. Holloway and E. G. Hope, *J. Fluorine Chem.*, 1996, **76**, 209-212.
15 K. Fagnou and M. Lautens, *Angew. Chem. Int. Ed.*, 2002, **41**, 26-47.
16 (*a*) E. W. Dahl, H. T. Dong and N. K. Szymczak, *Chem. Commun.*, 2018, **54**, 892-895; (*b*) C. M. Moore and N. K. Szymczak, *Chem. Commun.*, 2015, **51**, 5490-5492.
17 (*a*) Z. Thammavongsy, M. E. LeDoux, A. G. Breuhaus-Alvarez, T. Seda, L. N. Zakharov and J. D. Gilbertson, *Eur. J. Inorg. Chem.*, 2013, **2013**, 4008-4015. (*b*) G. A. N. Felton, R. S. Glass, D. L. Lichtenberger and D. H. Evans, *Inorg. Chem.*, 2006, **45**, 9181-9184
18 The solution state structure could not be assigned due to overlapping peaks in diamagnetic region of the ^{1}H NMR spectrum.
19 (*a*) M. M. da Mota, J. Rodgers and S. M. Nelson, *J. Chem. Soc. A*, 1969, **0**, 2036-2044; (*b*) T. Matsumoto, T. Nagahama, J. Cho, T. Hizume, M. Suzuki and S. Ogo, *Angew. Chem. Int. Ed.*, 2011, **50**, 10578-10580; (*c*) K. Takashita, T. Matsumoto, T. Yatabe, H. Nakai, M. Suzuki and S. Ogo, *Chem. Lett.*, 2016, **45**, 72-74.
20 A. Casitas, M. Canta, M. Solà, M. Costas and X. Ribas, *J. Am. Chem. Soc.*, 2011, **133**, 19386-19392.
21 J. Chatt and R. G. Hayter, *J. Chem. Soc.*, 1961, 772.
22 T. Steiner, *Angew. Chem. Int. Ed.*, 2002, **41**, 48-76.
23 J. W. Steed and J. L. Atwood, *Supramolecular Chemistry*, Wiley, West Sussex, 2nd edn., 2009.
24 P. V. Huong and M. Schlaak, *Chem. Phys. Lett.*, 1974, **27**, 111-113.
25 (*a*) L. Brammer, E. A. Bruton and P. Sherwood, *Cryst. Growth Des.*, 2001, **1**, 277-290; (*b*) P. R. Andrews, S. L. A. Munro, M. Sadek and M. G. Wong, *J. Chem. Soc., Perkin Trans. 2*, 1988, 711-718; (*c*)K. H. Moller, A. Kjaersgaard, A. S. Hansen, L. Du and H. G. Kjaergaard, *J. Phys. Chem. A*, 2018, **122**, 3899-3908.
26 (*a*) E. Szajna-Fuller, B. M. Chambers, A. M. Arif and L. M. Berreau, *Inorg. Chem.*, 2007, **46**, 5486-5498; (*b*) E. Szajna, P. Dobrowolski, A. L. Fuller, A. M. Arif and L. M. Berreau, *Inorg. Chem.*, 2004, **43**, 3988-3997.
27 Cambridge Structural Database, Version 5.41, October 2020; Cambridge Crystallographic Data Centre, 12 Union Road, Cambridge CB2 1EZ U.K.
28 (*a*) I. E. Soshnikov, N. V. Semikolenova, K. P. Bryliakov, A. A. Antonov, W.-H. Sun and E. P. Talsi, *J. Organomet. Chem.*, 2019, **880**, 267-271; (*b*) K. M. Arendt and A. G. Doyle, *Angew. Chem. Int. Ed.*, 2015, **54**, 9876-9880; (*c*) M. P. Suh, K. Y. Oh, J. W. Lee and Y. Y. Bae, *J. Am. Chem. Soc.*, 1996, **118**, 777-783.
29 A. W. Addison, T. N. Rao, J. Reedijk, J. van Rijn and G. C. Verschoor, *J. Chem. Soc., Dalton Trans.*, 1984, 1349-1356.
30 We attempted to identify ν_{NH} by IR spectroscopy; unfortunately, the bands are not sufficiently resolved enough to include a definitive commentary on H-bonding interactions in the reduced complexes (see ESI).
31 We acknowledge that the geometric change from O_h to TBP can have a similar effect in the shortening of H-bonding contacts and can contribute to the change observed here.
32 (*a*) L. Manojlovic-Muir, K. W. Muir, W. M. Davis, H. A. Mirza and R. J. Puddephatt, *Inorg. Chem.*, 1992, **31**, 904-909; (*b*) L. Sacconi, P. Dapporto and P. Stoppioni, *Inorg. Chem.*, 1977, **16**, 224-227.
33 (*a*) R. R. Gagne and D. M. Ingle, *Inorg. Chem.*, 1981, **20**, 420-425; (*b*) G. D. Jones, J. L. Martin, C. McFarland, O. R. Allen, R. E. Hall, A. D. Haley, R. J. Brandon, T. Konovalova, P. J. Desrochers, P. Pulay and D. A. Vicic, *J. Am. Chem. Soc.*, 2006, **128**, 13175-13183.
34 (*a*) C. C. Scarborough, K. M. Lancaster, S. DeBeer, T. Weyhermüller, S. Sproules and K. Wieghardt, *Inorg. Chem.*, 2012, **51**, 3718-3732; (*b*) P. J. Chirik and K. Wieghardt, *Science*, 2010, **327**, 794-795.
35 Due to the inability to isolate the reduced species, this value represents the maximum extinction coefficient, calculated from the concentration of [NiCl(TPA)]BAr'$_4$ prior to reduction.
36 S. Kannan, M. A. Moody, C. L. Barnes and P. B. Duval, *Inorg. Chem.*, 2006, **45**, 9206-9212.
37 M. B. Khaled, R. K. El Mokadem and J. D. Weaver, *J. Am. Chem. Soc.*, 2017, **139**, 13092-13101.
38 P. Erdmann, J. Leitner, J. Schwarz and L. Greb, *ChemPhysChem*, 2020, **21**, 987-994.
39 J. D. Yang, Y. Wang, X. S. Xue and J. P. Cheng, *J Org Chem*, 2017, **82**, 4129-4135.
40 We acknowledge the differences between the BDE (homolytic) and FIA (heterolytic) parameters. In contrast to the FIA parameters, the BDE values for these substrates have been reported, and provide one guiding metric.

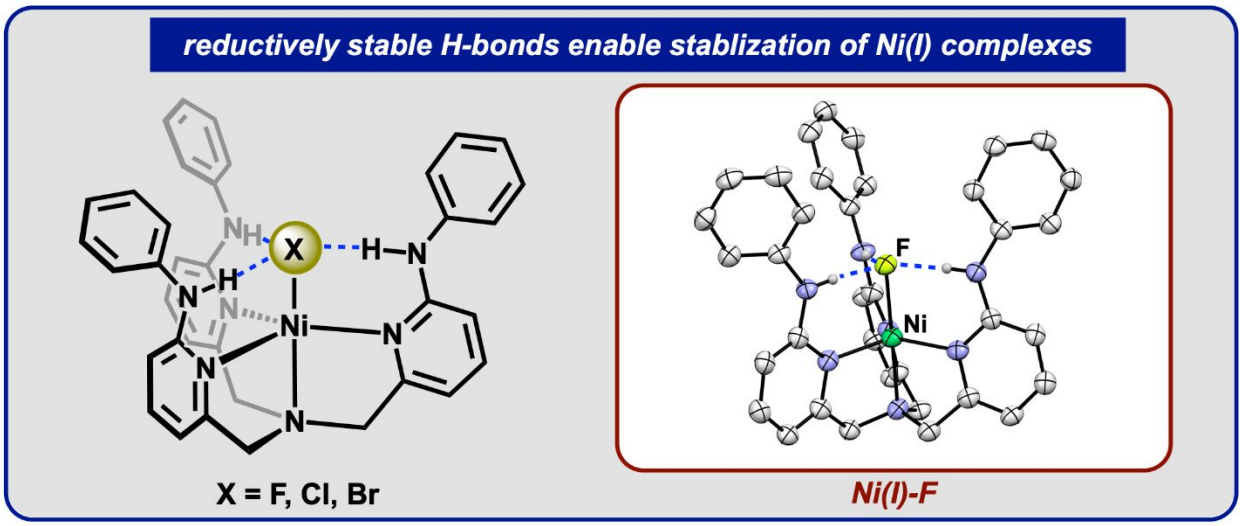

Secondary-sphere hydrogen bonds enable structural characterization and evaluation of an unusual nickel(I) fluoride complex.